ChemComm

COMMUNICATION

Alkoxylated dehydrobenzo[12]annulene on Au(111): From single molecules to quantum dot molecular networks[†]

Koen Schouteden,[*][a][¶] **Tsveta Ivanova,**[a][¶] **Zhe Li,**[a] **Violeta Iancu,**[a,b] **Kazukuni Tahara,**[c] **Yoshito Tobe,**[c] **Jinne Adisoejoso,**[d] **Steven De Feyter,**[d] **Chris Van Haesendonck,**[a] **and Ewald Janssens**[a]

We demonstrate the effective confinement of surface electrons in the pores of molecular networks formed by dehydrobenzo[12]annulene (DBA) molecules with butoxy groups (DBA-OC$_4$) on Au(111). Investigation of the network formation starting from single molecules reveals a considerable interaction of the molecules with the substrate, which is at the origin of the observed confinement.

Molecules have the extraordinary capability to self-organize on surfaces and create two-dimensional (2D) molecular crystals. By tuning the intermolecular and the molecule-substrate interactions one can create various molecular self-assemblies at surfaces like porous networks or close-packed layers. Self-assembled molecular networks in general have great appeal to fundamental science and promise towards new nano- and biotechnological devices[1–3] for various applications such as for memory, sensor and spintronic applications[4,5]. In particular, the porous molecular networks are very interesting systems because they provide nanometer sized voids (pores) in a highly organized 2D arrangement. These voids permit access to the underlying surface and provide ways to locally and periodically decorate the surface with nano-objects. In addition, the confinement of the surface electrons inside such voids will allow the creation of regular arrays of quantum dots with a rich and versatile electronic structure[6–9]. The electronic structure of the dots can be tuned by varying the size of the nanopores and the strength of the intermolecular interactions. Electronic confinement in porous structures has been

already demonstrated for networks formed via H-bonds[6], covalent bonds[10] or metal coordination bonds[3], but not for networks built via van-der Waals interactions.

DBA-based molecules, which consist of a triangular core with three benzene rings, have previously been investigated upon porous network formation at the liquid-solid interface, mostly on graphite surfaces, using scanning tunneling microscopy (STM)[11,12]. DBA porous molecular networks have already been successfully used to trap a variety of guest molecules in the pores[13]. More recently, porous networks of DBA and DBA-OC$_4$ molecules that are built via intermolecular van-der Waals interactions on Au(111) have also been studied in ultra-high vacuum (UHV) conditions by STM[14,15]. The electronic properties of these networks and their potential as quantum dot arrays have, however, not been addressed yet.

In this study we investigated single DBA-OC$_4$ molecules adsorbed on Au (111) and their organization into molecular networks. The formation of large 2D molecular networks is achieved by post-annealing at a temperature close to the sublimation temperature of the molecules. The lateral confinement of the 2D surface state (SS) electrons of the Au substrate within the pores of the network is evidenced by scanning tunneling spectroscopy (STS), illustrating the potential of DBA networks to generate highly ordered quantum dot arrays.

All experiments are conducted in a UHV (base pressure in the 10^{-11} mbar range) system that includes an Omicron low-temperature STM operated at 4.5 K. Au(111) films grown on mica are cleaned by Ar$^+$ sputtering and annealing cycles[16]. DBA-OC$_4$ is synthesized as described in Ref.[14]. DBA-OC$_4$ powder is sublimated at 480 K using a Knudsen cell and dosed onto the Au(111) substrate held at room temperature. For STM tips we used mechanically cut PtIr (10% Ir) and polycrystalline W wires. The W tips are electrochemically etched and cleaned in situ by thermal treatment. All bias voltages mentioned are with respect to the sample, and the STM tip is virtually grounded. The STM images are analyzed using the Nanotec WSxM software[17].

Figure 1 (a) presents an STM topography of the Au(111) surface after low-coverage DBA-OC$_4$ deposition at room tem-

perature (deposition time: 1 minute). Only single DBA-OC$_4$ molecules are retrieved and no networks are formed. It can be observed in Fig. 1 (a) that the single DBA-OC$_4$ molecules are preferentially adsorbed on the face-centered-cubic (fcc) regions of the herringbone reconstructed Au(111) surface. Only few molecules are present on the hexagonal-close-packed (hcp) regions and no molecules on the herring-bone ridges between the fcc and hcp regions of the Au(111) surface. This may be explained by the small electronic potential energy difference that exists between the reconstruction regions (the potential in hcp regions is about 25 meV lower than that in fcc regions[18]). The observation of individual molecules points to a low mobility, which may be due to their large size or due to a high diffusion barrier. However, the molecules must have a certain mobility, since they are able to move from their random landing position towards a Au(111) fcc region.

It can be seen in Figs. 1 (a) and (b) that the single molecules have a triangularly shaped appearance, reflecting the triangularly shaped DBA core of the DBA-OC$_4$ molecule. The single molecules have two different orientations on the Au(111) surface that are rotated by 60° with respect to each other [highlighted by the blue triangles in Fig. 1 (c)], reflecting the symmetry directions of the Au(111) support, similar to DBA molecules (without OC$_x$ legs) on Au(111)[15]. Remarkably, for each single DBA-OC$_4$ molecule one of the "corners" of the observed triangular shape appears higher than the other two "corners", suggesting that the single molecules adhere a tilted conformation on Au(111), which is in contrast to DBA molecules without OC$_x$ legs on Au(111)[15]. This may indicate that the legs of the DBA-OC$_4$ molecule are not parallel to the Au(111) surface. Alternatively, the tilted conformation may be related to the incommensurability of the molecule with the substrate. The tilted conformation of the single DBA-OC$_4$ molecules on Au(111) can be modified by locally applying a moderate voltage pulse, as illustrated in Fig. 1 (b). Successful "reorientation" is witnessed as a sudden jump in the recorded tunneling current during STS measurements [typical STS spectra are presented in Fig. S2 in the Supporting Information (SI)]. A reorientation already occurs for pulses above 0.5 V and the success rate increases with increasing voltage. Uncontrolled reorientation of the molecules also occurs during STM imaging at these voltages. Tip-induced lateral displacement of the single molecules did not occur in our experiments, indicating a considerable molecule-substrate interaction and/or diffusion barrier of the molecule on (the fcc regions of the) Au(111)[19]. Occasionally, a single DBA-OC$_4$ molecule with planar conformation is retrieved. For such planar conformation the six butoxy legs of the molecule can be nicely resolved [see inset of Fig. 1 (a)]. A chemical model structure of DBA-OC$_4$ is superimposed on the image (see Fig. S1 in the SI for enlarged view). The apparent (maximum) height of the tilted molecule on Au(111) is 0.24 ± 0.01 nm,

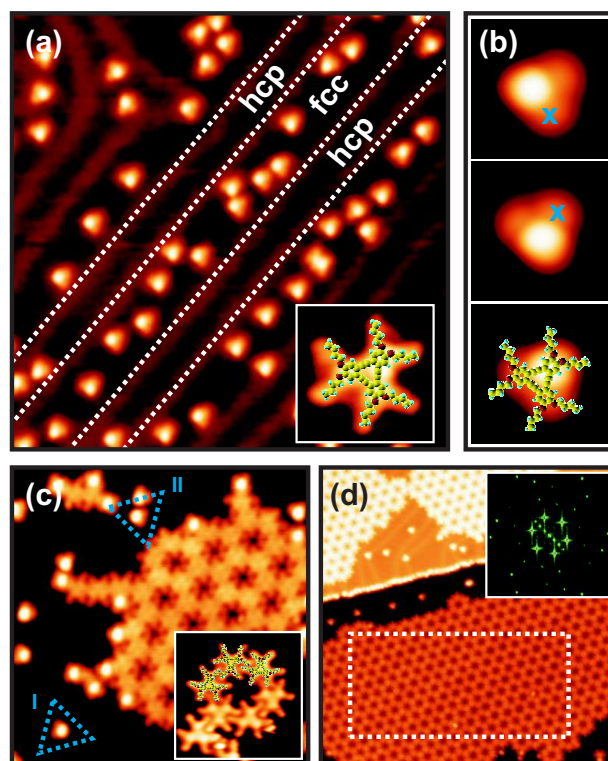compared to 0.15 ± 0.01 nm for the planar molecule.

Fig. 1 (a) 30×30 nm^2 STM topography of individual DBA-OC$_4$ molecules with tilted conformation on Au(111) at low coverage. $V = +0.20$ V; $I = 0.01$ nA. Inset: 3×3 nm^2 close-up view of a DBA-OC$_4$ molecule with planar conformation. (b) Sequence of 3×3 nm^2 STM topographies (top to bottom) of the same DBA-OC$_4$ molecule with three different tilted conformations. The tilt conformation is changed from one to the other by a applying a local voltage pulse at the indicated location (blue crosses). $V = -0.30$ V; $I = 0.5$ nA. (c) 22×22 nm^2 STM topography of DBA-OC$_4$ molecules on Au(111) at higher coverage for which small network formation occurs. $V = -0.15$ V; $I = 0.05$ nA. Inset: Close-up view of a nanopore with a radius of 1.90 nm. (d) Annealing to 460 K further promotes the formation of large networks. $V = +0.50$ V; $I = 0.02$ nA. Image size is 70×70 nm^2. Inset: 2.7×2.7 nm^{-2} Fourier-transform of the area enclosed by the dashed rectangle highlights the hexagonal organization of the molecules. 1D-maxima stem from the reconstruction of the underlying Au(111).

Upon increasing the amount of molecules (deposition time: five minutes), very small networks can be retrieved [see Fig. 1 (c)]. The networks exhibit nanosized pores and have a hexagonal structure, consistent with previous findings[14]. Remarkably, DBA-OC$_4$ molecules that contribute to a nanoporous network favor planar conformations, in particular molecules that are part of a complete hexagon. This is illustrated in the high-resolution[20] inset of Fig. 1 (c), on which 3 model structures of DBA-OC$_4$ are superimposed. Several

molecules located at the border of the network and that are not part of a complete hexagons still exhibit a tilted conformation, probably due to the missing neighbor(s). Moderate annealing to 370 K for 90 minutes does not result in noticeable diffusion effects. Annealing to about 460 K (close to the sublimation temperature of the molecules) for about 90 minutes is required to promote the formation of large networks of over 100 nm in size [see Fig. 1 (d)]. Both clockwise and counterclockwise chirality structures are observed (see Fig. S4 in SI)[14].

Ref.[14] previously reported density functional theory (DFT) calculations of DBA-OC$_4$ molecules that reveal a pore radius r of 1.65 nm (measured from center of pore to center of molecule), i.e., a pore diameter d of 3.30 nm. The DFT result was in good agreement with the experimentally determined lattice constant $a = b = 2.9 \pm 0.1$ nm, corresponding to a pore diameter $d = a/\cos 30^o = 3.4 \pm 0.1$ nm. Here we find that the pore diameter is somewhat larger, i.e., $d = 3.8 \pm 0.1$ nm. The submolecular resolution in our STM topographies allows to clearly identify the organization of the molecules in the network. We find that is consistent with that reported in Ref.[14], which indicates that chain-chain van der Waals interactions are the dominant forces in the network formation. The discrepancy of our experimentally found pore diameter with the previously reported result may be related to variations of the Au(111) herringbone reconstruction, which can influence the precise assembly of the molecules. Such local modifications of the herringbone reconstruction can be induced by defects and steps that exist at the Au(111) surface, as well as by interactions with molecular adsorbates.

Next we investigated the electronic properties of the DBA-OC$_4$ molecules on Au(111). The $(dI/dV)(V)$ spectrum of the (planar) DBA-OC$_4$ molecules in the network in Fig. 2 (d) exhibits a pronounced resonance around -0.75 V, which can be assigned to the highest occupied molecular orbital (HOMO) of the molecule. In contrast, the spectrum of individual (tilted) DBA-OC$_4$ molecules is more or less featureless and often suffers from instabilities related to its voltage-induced reorientation. Voltage-dependent STM imaging reveals an increase of the apparent height of the molecules in the 2.5 to 3.5 V range, i.e., from 0.12 ± 0.03 nm to 0.15 ± 0.03 nm (see Fig. S3 in the SI). This is a significant increase when considering the increasing tip convolution effects with increasing voltage[21]. The increased apparent height is accompanied by a (small) change of the appearance of the molecules. This voltage-dependent behavior may be explained by orbital-mediated tunneling[22] and points to the existence of the lowest unoccupied molecular orbital (LUMO) of DBA-OC$_4$ around 3.0 V. When compared to DBA on Au(111)[15], this implies that the OC$_4$ groups do not strongly affect the HOMO-LUMO gap of DBA on Au(111), i.e., both HOMO and LUMO are shifted to higher energies by about 1 eV for DBA-OC$_4$ on Au(111).

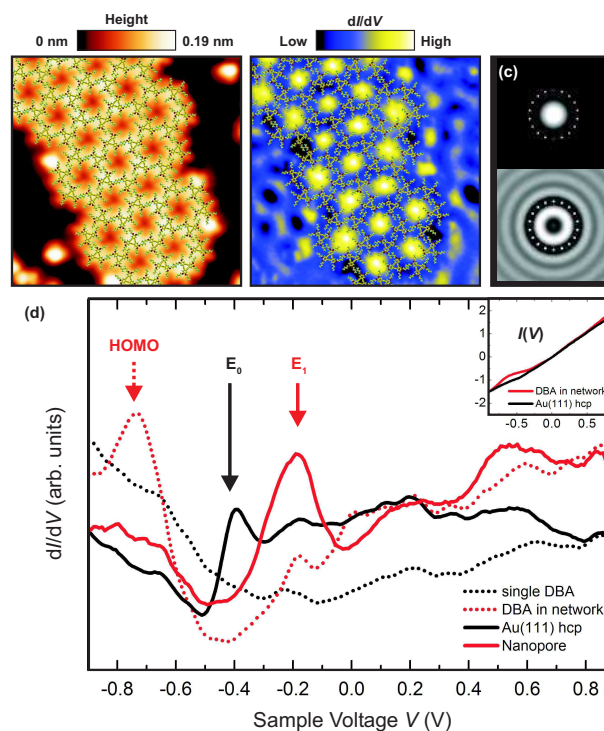To quantify the electron confinement capacity of the DBA-

Fig. 2 (a) 18×18 nm^2 STM topography and (b) the corresponding constant-current dI/dV map. $V = -0.15$ V; $I = 0.05$ nA. A schematic model structure of the molecular network is superimposed on both images. (c) Particle-in-a-box dI/dV map simulations for a circular box[23] at -0.15 eV (top) and $+0.80$ eV (bottom). (d) Open feedback loop (dI/dV)(V) spectra of individual DBA-OC$_4$, of DBA-OC$_4$ in the network, and of the pores. A spectrum of the surrounding bare Au(111) is added as a reference. Each spectrum is the average of 10 spectra recorded on different locations (molecules/pores). Spectra are recorded with lock-in detection using an amplitude of 20 mV and a frequency of 800 Hz. Inset: $I(V)$ spectra of DBA-OC$_4$ in the network and of Au(111). Setpoints are $V = -0.90$ V and $I = 0.50$ nA.

OC$_4$ network we measured the electronic structure in the pores using (dI/dV)(V) spectra and compared with that of the surrounding substrate. The (dI/dV)(V) spectrum of the nanopores in the network exhibits a pronounced resonance around -190 meV [see Fig. 2 (d)]. The resonance energy is about the same for each pore. This resonance points to the existence of quantum confinement effects in the pores, i.e., the molecules surrounding the pore act as an effective potential barrier for the 2D SS electrons of the Au(111) surface. This localization creates discrete energy levels inside the pores. A (dI/dV)(V) spectrum of the surrounding bare Au(111), showing the step-like onset of the Au SS at E_0 = -460 meV, is added as a reference[16]. To a simplest approximation, the electron confinement inside the pore can be modeled by a circular shaped box

following the 2D particle-in-a-box model:

$$E_N = E_0 + \frac{\lambda_N}{m^*\Omega} \qquad N = 1, 2, 3, ..., \qquad (1)$$

where Ω is the effective area of the confining surface, and λ_N denotes the eigenvalues that depend solely on the shape of the box. For a finite height of the confining potential, Ω can become somewhat larger than the actual surface area of the nanoparticle because of "spill-out" of the particle's wavefunctions[24,25]. The resonance in the pores reflects the first eigenstate of the nanopore with eigenenergy $E_1 = -190$ meV[26]. The nanoporous network can thus be considered as a regular array of quantum dots[6,9].

The first eigenstate of the nanopores is visualized by the bright maxima in the dI/dV map in Fig. 2 (b), of which the corresponding topography is presented in Fig. 2 (a). Standing waves can also be resolved outside the network patch in Fig. 2 (b), again indicating that the molecules are an effective scattering center for the Au(111) SS electrons. At $V = 800$ mV a ring of higher intensity with a local minimum at its center can be observed in the pores in the dI/dV maps (see Fig. S5 in the SI). No clear standing-wave patterns are observed in the pores at more elevated voltages, which is related to the very complex shape of the pore yet also to intrinsic tip convolution effects due to the finite size of the STM tip.

A value for the effective confining area of the nanopores can be inferred from simulations using the particle-in-a-box software (available via Ref.[23]) developed by K.-F. Braun[27] (the Schrödinger equation is solved by treating adatom scattering centers as zero-range potentials). Taking $E_0 = -460$ meV and the effective electron mass $m^* \approx 0.23 m_e$[16], we find good agreement with the circular box model when taking a diameter of 3.8 nm [see simulated dI/dV maps Fig. 2 (c)]. The good agreement between the simulations in Fig. 2 (c) and the experiments supports interpretation of the results in terms of particle-in-a-box type confinement. We note that the diameter value in the simulations is the same as the experimentally determined pore diameter and therefore interaction between the nanopore quantum dots may exist. However, within our series of experiments we did not observe a coupling between the quantum dots. In situ photoemission experiments may be better suited for the investigation of QD coupling[6,9], yet such experiments are beyond the scope of our present work.

In conclusion, network formation of DBA-OC$_4$ molecules on Au(111) is investigated, starting from single molecules to large nanoporous networks that are built through van der Waals intermolecular interactions. The nanopores reveal pronounced particle-in-box-type confinement of the Au surface state. Our findings open perspectives for use of DBA-derivatives for obtaining highly ordered quantum dot arrays.

References

1 J. V. Barth, *Annu. Rev. Phys. Chem.*, 2007, **58**, 375407.

2 Y. Pennec, W. Auwärter, A. Schiffrin, A. Weber-Bargioni, A. Riemann and J. V. Barth, *Nature Nanotech.*, 2007, **2**, 99.

3 S. Nowakowska, A. Wäckerlin, S. Kawai, T. Ivas, J. Nowakowski, S. Fatayer, C. Wäckerlin, T. Nijs, E. Meyer, J. Björk, M. Stöhr, L. H. Gade and T. A. Jung, *Nature Commun.*, 2015, **6**, 6071.

4 L. Bogani and W. Wernsdorfer, *Nature Mater.*, 2008, **7**, 179–186.

5 W. Auwärter, D. Écija, F. Klappenberger and J. V. Barth, *Nat. Chem.*, 2015, **7**, 105–120.

6 J. Lobo-Checa, M. Matena, K. Müller, J. H. Dil, F. Meier, L. H. Gade, T. A. Jung and M. Stöhr, *Science*, 2009, **325**, 300.

7 F. Klappenberger, D. Kuühne, W. Krenner, I. Silanes, A. Arnau, F. García de Abajo, S. Klyatskaya, M. Ruben and J. V. Barth, *Nano Lett.*, 2009, **9**, 3509–3514.

8 A. Shchyrba, S. C. Martens, C. Wäckerlin, M. Matena, T. Ivas, H. Wadepohl, M. Stöhr, T. A. Jung and L. H. Gade, *Chem. Commun.*, 2014, **50**, 7628–7631.

9 N. Kepcija, T.-J. Huang, F. Klappenberger and J. V. Barth, *J. Chem. Phys.*, 2015, **142**, 101931.

10 L. Grill, M. Dyer, L. Lafferentz, M. Persson, M. V. Peters and S. Hecht, *Nat. Nanotech.*, 2007, **2**, 687–691.

11 K. Tahara, H. Yamaga, E. Ghijsens, K. Inukai, J. Adisoejoso, M. O. Blunt, S. D. Feyter and Y. Tobe, *Nature Chem.*, 2011, **3**, 714–719.

12 B. Li, K. Tahara, J. Adisoejoso, W. Vanderlinden, K. S. Mali, S. D. Gendt, Y. Tobe and S. D. Feyter, *ACS Nano*, 2013, **7**, 1076410772.

13 E. Ghijsens, H. Cao, A. Noguchi, O. Ivasenko, Y. Fang, K. Tahara, Y. Tobe and S. D. Feyter, *Chem. Commun.*, 2015, **51**, 4766.

14 J.-H. Kim, K. Tahara, J. Jung, S. De Feyter, Y. Tobe, Y. Kim and M. Kawai, *J. Phys. Chem. C*, 2012, **116**, 17082–17088.

15 J.-H. Kim, J. Jung, K. Tahara, Y. Tobe, Y. Kim and M. Kawai, *J. Chem. Phys.*, 2014, **140**, 074709.

16 K. Schouteden, P. Lievens and C. Van Haesendonck, *Phys. Rev. B*, 2009, **79**, 195409.

17 I. Horcas, R. Fernandez, J. M. Gomez-Rodriguez, J. Colchero, J. Gomez Herrero and A. M. Baro, *Rev. Sci. Instrum.*, 2007, **78**, 013705.

18 W. Chen, V. Madhavan, T. Jamneala and M. F. Crommie, *Phys. Rev. Lett.*, 1998, **80**, 1469–1472.

19 Stable imaging is achieved for voltages in the 0.1 to 0.5 V range when using low tunneling currents in the 0.01 to 0.1 nA range.

20 Such high-resolution images are obtained with an STM tip that has been modified by picking up a (fraction of a) DBA molecule with the STM tip.

21 The tip-sample distance increases with increasing tunneling voltage when keeping the tunneling current fixed and leads to increased tip convolution.

22 V. Iancu, K.-F. Braun, K. Schouteden and C. Van Haesendonck, *Langmuir*, 2013, **29**, 11593–11599.

23 K.-F. Braun, Calculation of Standing Wave Pattern and Image Processing http://www.kai-felix-braun.de/program.htm (2006).

24 J. Li, W.-D. Schneider, R. Berndt and S. Crampin, *Phys. Rev. Lett.*, 1998, **80**, 3332.

25 J. Zhang, A. Shchyrba, S. Nowakowska, E. Meyer, T. A. Jung and M. Muntwiler, *Chem. Commun.*, 2014, **50**, 12289–12292.

26 D. J. Griffiths, *Introduction to quantum mechanics*, Prentice-Hall, 1995, pp. 274–283.

27 K.-F. Braun and K.-H. Rieder, *Phys. Rev. Lett.*, 2002, **88**, 096801.